Modeling of the Copolymerization Kinetics of n-Butyl Acrylate and d-Limonene Using PREDICI ®

Authors:

Shanshan Ren, Eduardo Vivaldo-Lima, Marc A. Dubé

Date Submitted: 2018-07-30

Keywords: Modelling, polymerization kinetics, n-butyl acrylate, d-limonene

Abstract:

Kinetic modeling of the bulk copolymerization of d-limonene (Lim) and n-butyl acrylate (BA) at 80 °C was performed using PREDICI®. Model predictions of conversion, copolymer composition and average molecular weights are compared to experimental data at five different feed compositions (BA mol fraction = 0.5 to 0.9). The model illustrates the significant effects of degradative chain transfer due to the allylic structure of Lim as well as the intramolecular chain transfer mechanism due to BA.

Record Type: Published Article

Submitted To: LAPSE (Living Archive for Process Systems Engineering)

Citation (overall record, always the latest version):	LAPSE:2018.0151
Citation (this specific file, latest version):	LAPSE:2018.0151-1
Citation (this specific file, this version):	LAPSE:2018.0151-1v2

DOI of Published Version: https://doi.org/10.3390/pr4010001

processes

MDPI

Article

Modeling of the Copolymerization Kinetics of *n*-Butyl Acrylate and D-Limonene Using PREDICI ®

Shanshan Ren [1], Eduardo Vivaldo-Lima [2] and Marc A. Dubé [1,*]

Received: 29 November 2015; Accepted: 16 December 2015; Published: 24 December 2015
Academic Editor: Masoud Soroush

[1] Department of Chemical and Biological Engineering, Centre for Catalysis Research and Innovation, University of Ottawa, 161 Louis Pasteur Pvt., Ottawa, ON K1N 6N5, Canada; sren051@uottawa.ca
[2] Facultad de Química, Departamento de Ingeniería Química, Universidad Nacional Autónoma de México, México D.F. 04510, Mexico; vivaldo@unam.mx
* Correspondence: marc.dube@uottawa.ca; Tel.: +1-613-562-5915; Fax: +1-613-562-5174

Abstract: Kinetic modeling of the bulk copolymerization of D-limonene (Lim) and *n*-butyl acrylate (BA) at 80 °C was performed using PREDICI®. Model predictions of conversion, copolymer composition and average molecular weights are compared to experimental data at five different feed compositions (BA mol fraction = 0.5 to 0.9). The model illustrates the significant effects of degradative chain transfer due to the allylic structure of Lim as well as the intramolecular chain transfer mechanism due to BA.

Keywords: modeling; polymerization kinetics; *n*-butyl acrylate; D-limonene

1. Introduction

Due to environmental constraints and the need to reduce human dependence on fossil resources, the use of renewable chemical compounds and the incorporation of a naturally-occurring carbon framework into polymer chains has attracted great interest [1,2]. As one of the largest class of renewable feedstocks, terpenes present great potential to replace fossil-based chemical compounds because of their low toxicity, abundant production, and significantly low contribution to the carbon cycle [3–5]. D-limonene (Lim) is a cyclic monoterpene which consists of one isoprene (C_5H_8) unit and is obtained as a by-product from the orange juice industry. For all practical purposes, the free-radical homopolymerization of Lim is not possible. However, the free-radical copolymerization of Lim with various monomers, such as *n*-butyl acrylate (BA) [6], butyl methacrylate (BMA) [7], 2-ethyl hexyl acrylate (EHA) [8], *etc.*, has been reported. In our previous studies [6,9], it was shown that degradative chain transfer due to the presence of Lim competed remarkably with chain propagation. The suppression of both rate of polymerization and molecular weight development were observed. In order to get better insight on the mechanism and the corresponding kinetic parameters related to Lim, a comprehensive model of free-radical copolymerization of BA/Lim was developed using the PREDICI ® simulation package. The model is an extension of previous efforts for the BMA/Lim and EHA/Lim systems [10]. The current effort includes further refinement of the Lim rate parameters and addition of an intramolecular chain transfer (*i.e.*, back-biting) mechanism for BA.

BA is a common monomer that is widely used in coating and adhesive formulations due to its excellent resistance to water, solvent and sunlight, as well as the transparency and low-temperature flexibility of its polymer. The mechanism and kinetic parameters of BA have been well-studied for various homo- and copolymerization systems. Recently, it has been reported that the polymerization rate of BA measured by the pulsed-laser polymerization (PLP) method is much slower than expected for chain-end propagation, and this is due to the intramolecular chain-transfer of BA (also referred to

as backbiting) yields tertiary radicals which present much slower propagation rates than the typical secondary radicals resulting from chain-end propagation [11–13]. The backbiting mechanism was considered in this work, and the corresponding parameters were mainly taken from Hutchinson and Rantow's work [11,14–17]. Other basic kinetic parameters used in this work were obtained from the WATPOLY database from the University of Waterloo [18–20], which contains parameters for a wide range of monomers, initiators, solvents, CTAs, *etc.*, and can provide good predictions on polymerization rate, composition, and molecular weight in bulk/solution/emulsion systems under a broad range of reaction conditions.

2. Experimental Section

The polymerization conditions and experimental data used herein are from a previous experimental study of the BA/Lim system [6]. Several bulk copolymerizations for five separate BA/Lim feed concentrations were conducted at 80 °C using benzoyl peroxide (BPO) (Sigma-Aldrich, Oakville, ON, Canada) as the initiator. Polymerizations were performed in glass ampoules in an oil bath. Oxygen was removed using several freeze-pump-thaw cycles. Monomer conversion was determined by gravimetry; copolymer composition was measured by ^{1}H-NMR spectroscopy (400 MHz, Bruker Avance, Billerica, MA, USA); and average molecular weights and distribution were obtained by gel permeation chromatography (GPC) (Agilent/Wyatt Technology, Santa Clara/Santa Barbara, CA, USA) equipped with a multi-angle light scattering detector, a differential refractive index detector and a differential viscometer. The initial monomer and initiator concentrations are shown in Table 1.

Table 1. Experimental conditions for BA/Lim bulk polymerization at 80 °C.

Monomer Feed (BA Molar Fraction)	BA (mol L^{-1})	Lim (mol L^{-1})	BPO (mol L^{-1})
f_{BA} = 0.9	6.13	0.68	0.036
f_{BA} = 0.8	5.38	1.35	0.036
f_{BA} = 0.7	4.65	2.00	0.036
f_{BA} = 0.6	3.91	2.67	0.036
f_{BA} = 0.5	3.26	3.26	0.036

3. Model Development

The polymerization mechanism was implemented in PREDICI ® and was based on conventional free-radical bulk copolymerization kinetics. Equations describing intramolecular chain transfer (BA) and degradative chain transfer (Lim) were added to the mechanism. Parameter values were taken initially from the literature (including from our previous modeling work on BMA/Lim [10]). The only parameters adjusted were the homopropagation rate constants for BA and Lim. The model equations and initial and final parameter values are shown in Table 2. In Table 2, unreferenced initial parameters were initial guesses for the parameters.

Table 2. Polymerization mechanism and kinetic rate constants used for the PREDICI ® simulation of the bulk free-radical copolymerization of BA/Lim at 80 °C [a].

Description	Step in PREDICI ®	Variables	Initial Value (L mol^{-1} s^{-1} Unless Otherwise Stated)
Initiation			
Initiator decomposition	I→2fR$^{\bullet}$	k_d, f	$k_d = 2.52 \times 10^{-5}$ s^{-1} [21], f = 0.6
First propagation to Lim	R$^{\bullet}$ + M$_1$→Lim$^{\bullet}$	k_{i1}	1.3 [10], adjusted value = 0.325
First propagation to BA	R$^{\bullet}$ + BA→BA$^{\bullet}$	k_{i2}	4.97×10^4 [17,22]
Propagation			
Self-propagation of Lim	PLim(s)$^{\bullet}$ + Lim→PLim (s + 1)$^{\bullet}$	k_{p11}	1.3 [10], adjusted value = 0.325
Cross-propagation	PLim(s)$^{\bullet}$ + BA→PBA (s + 1)$^{\bullet}$	k_{p12}	19.9, adjusted value = 48.5
Self-propagation of BA	PBA(s)$^{\bullet}$ + BA→PBA (s + 1)$^{\bullet}$	k_{p22}	4.97×10^4 [17,22], adjusted value = 2.49×10^5
Cross-propagation	PBA(s)$^{\bullet}$ + Lim→PLim (s + 1)$^{\bullet}$	k_{p21}	8.2×10^3, adjusted value = 4.10×10^4

Table 2. *Cont.*

Description	Step in PREDICI ®	Variables	Initial Value (L mol^{-1} s^{-1} Unless Otherwise Stated)
Chain transfer			
Chain transfer to BA	PLim(s)$^{\bullet}$ + BA→P(s) + BA$^{\bullet}$	k_{fm12}	1.44×10^{-2}
Chain transfer to BA	PBA(s)$^{\bullet}$ + BA→P(s) + BA$^{\bullet}$	k_{fm22}	3.68×10^{-1} [21]
Degradative chain transfer	PLim(s)$^{\bullet}$ + Lim→P(s) + ALim$^{\bullet}$	k_{fm11}	4.65×10^{-1}
Degradative chain transfer	PBA(s)$^{\bullet}$ + Lim→P(s) + ALim$^{\bullet}$	k_{fm21}	2.93×10^{2}
Re-initiation of ALim$^{\bullet}$	ALim$^{\bullet}$ + Lim→Lim$^{\bullet}$	k_{ra1}	1.67×10^{-10} [10]
Re-initiation of ALim$^{\bullet}$	ALim$^{\bullet}$ + BA→BA$^{\bullet}$	k_{ra2}	1.67×10^{-8} [10]
Termination			
By combination	PLim(s)$^{\bullet}$ + PLim(r)$^{\bullet}$→P(s + r)	k_{tc11}	1.79×10^{8}
-	PLim(s)$^{\bullet}$ + PBA(r)$^{\bullet}$→P(s + r)	k_{tc12}	1.79×10^{8}
-	PBA(s)$^{\bullet}$ + PBA(r)$^{\bullet}$→P(s + r)	k_{tc22}	1.79×10^{8} [14,17]
-	ALim$^{\bullet}$ + ALim$^{\bullet}$→AA	k_{tcaa}	9.95×10^{7}
-	PLim(s)$^{\bullet}$ + ALim$^{\bullet}$→P(s)	k_{tc1a}	1.79×10^{8}
-	PBA(s)$^{\bullet}$ + ALim$^{\bullet}$→P(s)	k_{tc2a}	1.79×10^{8}
By disproportionation	PLim(s)$^{\bullet}$ + PLim(r)$^{\bullet}$→P(s) + P(r)	k_{td11}	1.99×10^{7}
-	PLim(s)$^{\bullet}$ + PBA(r)$^{\bullet}$→P(s) + P(r)	k_{td12}	1.99×10^{7}
-	PBA(s)$^{\bullet}$ + PBA(r)$^{\bullet}$→P(s) + P(r)	k_{td22}	9.95×10^{7} [14,17]
Intramolecular chain transfer of BA			
Backbiting of BA	PBA(s)$^{\bullet}$→QBA(s)$^{\bullet}$	k_{bb}	5.76×10^{3} [16,21]
Short-chain branching	QBA(s)$^{\bullet}$+Lim→PLim(s+1)$^{\bullet}$	$k_{p21}{}^{tert}$	8.23
Short-chain branching	QBA(s)$^{\bullet}$+BA→PBA(s+1)$^{\bullet}$	$k_{p22}{}^{tert}$	49.9 [16,21]
Degradative chain transfer	QBA(s)$^{\bullet}$+Lim→P(s)+ALim$^{\bullet}$	$k_{fm2a}{}^{tert}$	1.83
Termination of BA tertiary radicals			
By combination (QBA$^{\bullet}$)	QBA(s)$^{\bullet}$ + QBA(r)$^{\bullet}$→P(s + r)	$k_{tc22}{}^{tert-tert}$	1.99×10^{7} [14,17]
-	QBA(s)$^{\bullet}$ + PBA(r)$^{\bullet}$→P(s + r)	$k_{tc22}{}^{tert-sec}$	5.97×10^{7} [14,17]
-	QBA(s)$^{\bullet}$ + PLim(r)$^{\bullet}$→P(s + r)	$k_{tc21}{}^{tert-sec}$	5.97×10^{7}
-	QBA(s)$^{\bullet}$ + ALim$^{\bullet}$→P(s)	$k_{tc2a}{}^{tert-a}$	9.95×10^{7}
By disproportionation (QBA$^{\bullet}$)	QBA(s)$^{\bullet}$ + QBA(r)$^{\bullet}$→P(s) + P(r)	$k_{td22}{}^{tert-tert}$	1.79×10^{8} [14,17]
-	QBA(s)$^{\bullet}$ + PBA(r)$^{\bullet}$→P(s) + P(r)	$k_{td22}{}^{tert-sec}$	1.39×10^{8} [14,17]
-	QBA(s)$^{\bullet}$ + PLim(r)$^{\bullet}$→P(s) + P(r)	$k_{td21}{}^{tert-sec}$	1.39×10^{8}
-	QBA(s)$^{\bullet}$ + ALim$^{\bullet}$→P(s) + A	$k_{td2a}{}^{tert-a}$	9.95×10^{7}

[a] R$^{\bullet}$ = initiator radical; BA and Lim = monomer units; BA$^{\bullet}$ and Lim$^{\bullet}$ = primary radicals; RBA(s)$^{\bullet}$ and RLim(r)$^{\bullet}$= polymer radicals of sizes s and r and ending in BA and Lim, respectively; ALim$^{\bullet}$ = allylic radicals resulting from degradative chain transfer of Lim; QBA$^{\bullet}$ = mid-chain tertiary radical from intramolecular chain transfer of BA; P(s) and P(r) = dead polymers.

3.1. Initiation

The initiation reaction involves two steps:

$$\mathrm{I} \xrightarrow{k_d} 2f\mathrm{R}^{\bullet} \tag{1}$$

$$\mathrm{R}^{\bullet} + \mathrm{M_i} \xrightarrow{k_{pii}} \mathrm{R_i}\,(1)^{\bullet} \tag{2}$$

Firstly, the homolysis of BPO initiator (I) yields a pair of primary radicals (R$^{\bullet}$). The decomposition rate of BPO is expressed by an Arrhenius relation, the pre-exponential factor and activation energy values were taken from the WATPOLY simulator database developed by Gao and Penlidis [18–21]:

$$k_d\ (\mathrm{s}^{-1}) = 1.07 \times 10^{14} \exp(-1.515 \times 10^{4}/T) \tag{3}$$

The primary radicals generated by the homolysis step then react with monomer and produce a chain-initiating radical, $\mathrm{R_i}(1)^{\bullet}$. However, not all initiator radicals can react with monomer, they may recombine, or abstract a proton from limonene. These factors were considered in the simulation by introducing an initiator efficiency factor (f). The value of f was set at 0.6, meaning 60% of the primary radicals produced by homolysis could initiate the polymerization.

3.2. Propagation

Using the terminal model, a total of four homo- and cross-propagation reactions were considered:

$$R_i\,(1)^{\bullet} + M_j \xrightarrow{k_{pij}} R_j\,(s+1)^{\bullet} \quad (4)$$

where k_{pij} is the rate constant of monomer j (M_j) adding to a propagating chain radical ending in monomer i. Note that in this work, 1 refers to limonene (Lim) and 2 refers to n-butyl acrylate (BA). The initially guessed propagation rate constant of BA was:

$$k_{p22}\ (\mathrm{L\ mol^{-1}s^{-1}}) = 2.21 \times 10^7 \exp(-2153/T) \quad (5)$$

The parameter values were taken from a comprehensive study of BA propagation rate constants using the pulsed-laser polymerization method [23]. The initially-guessed homopolymerization rate constant for Lim (k_{p11}) was taken from our previous modeling study of BMA/Lim copolymerization [10]. The cross-propagation rate constants, k_{p12} and k_{p21} were calculated from the reactivity ratios. Using terminal model kinetics, the reactivity ratios are defined as $r_i = \frac{k_{pii}}{k_{pij}}$. The values of r_1 = 0.0067 and r_2 = 6.007 were determined previously using low conversion bulk experiments at 80 °C [6]. As noted above, the homopropagation rate constants for BA and Lim were the only parameters adjusted in this work. Of course, because of the reactivity ratios, this also resulted in an adjustment to the cross-propagation rate constants.

3.3. Chain Transfer to BA and the Degradative Chain Transfer of Lim

In bulk polymerization, the influence of chain transfer to monomer on molecular weight cannot be ignored due to the high concentration of monomer. The chain transfer to BA is expressed as:

$$R_i\,(s)^{\bullet} + M_2 \xrightarrow{k_{fmij}} P\,(s) + R_2\,(1)^{\bullet} \quad (6)$$

The initially guessed rate constant for chain transfer to BA was taken from the WATPOLY database [21,23]:

$$k_{fm22}\ (\mathrm{L\ mol^{-1}s^{-1}}) = 1.56 \times 10^4 \exp(-3762/T) \quad (7)$$

As demonstrated in our previous study [6], the highly reactive allylic hydrogen of Lim can easily be abstracted by the growing polymer radical, and yield an inactive chain along with an allylic radical (see Scheme 1). Since the allylic radical is very stable, it is highly unlikely to initiate additional propagation; this mechanism is referred to as degradative chain transfer, and is the dominant chain transfer reaction in the BA/Lim system:

$$R_i\,(s)^{\bullet} + \mathrm{Lim} \xrightarrow{k_{fmi1}} P\,(s) + A_{Lim}{}^{\bullet} \quad (8)$$

$$\mathrm{ALim}^{\bullet} + M_i \xrightarrow{k_{r1i}} R_i\,(1) \quad (9)$$

Here the symbol $\mathrm{ALim}^{\bullet}$ was used to distinguish the allylic radical from the propagating Lim radical ($\mathrm{RLim}^{\bullet}$). To obtain an estimate of the chain transfer constant to Lim (C_s), the Mayo equation was used:

$$\frac{1}{\overline{X}_n} = \frac{1}{\overline{X}_{n0}} + C_s \frac{[S]}{[M]} \quad (10)$$

where C_s is defined as the ratio of the chain transfer to Lim rate constant to the BA propagation rate constant; that is, $C_s = \frac{k_{fm21}}{k_{p22}}$, $\overline{X}_n$ is the number-average degree of polymerization, $\overline{X}_{n0}$ is the number-average degree of polymerization in the absence of solvent/chain transfer agent, $[S]$ and $[M]$ are the molar concentrations of solvent/chain transfer agent and/or monomer, respectively. By plotting $\frac{1}{\overline{X}_n}$ *vs.* $\frac{[S]}{[M]}$, C_s was calculated from the slope as 4.9×10^{-3}. An assumption that Lim acts

more like a solvent or chain transfer agent rather than a propagating monomer was used to simplify the equation. The corresponding Mayo plot is given in Figure 1.

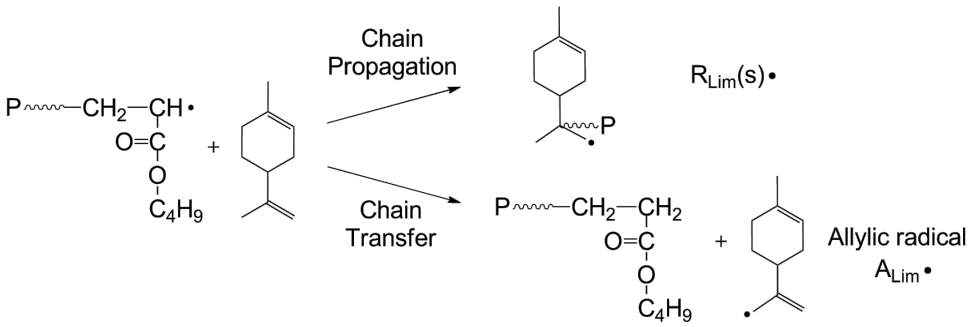

Scheme 1. Ideal reaction schematic of chain propagation and degradative chain transfer of Lim.

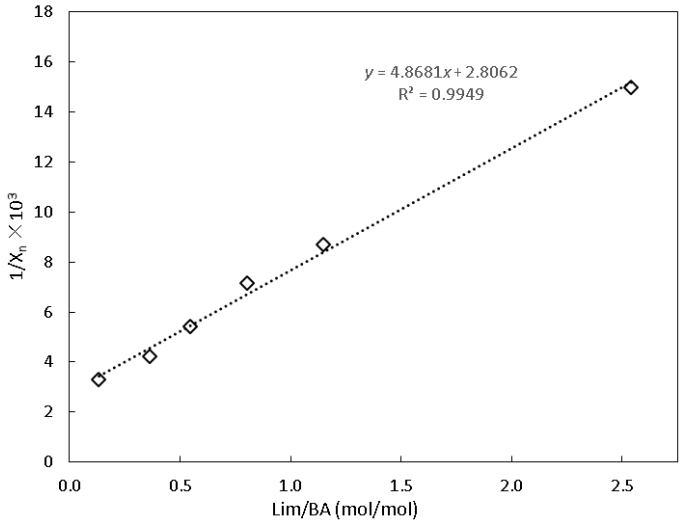

Figure 1. Mayo plot for the estimation of chain transfer constant to Lim (C_s).

To simplify the model, it is reasonable to assume the propagating radicals present the same chain transfer reactivity (*H*-atom abstraction) to a particular monomer as their propensity of adding to that monomer during propagation [11]. Accordingly, k_{fm21} and k_{fm12} were calculated as:

$$\frac{k_{fm21}}{k_{fm11}} = \frac{k_{p21}}{k_{p11}} \text{ and } \frac{k_{fm12}}{k_{fm22}} = \frac{k_{p12}}{k_{p22}} \tag{11}$$

The value of the re-initiation rate constant for the allylic radical was assumed to be very small as the radical is stable and would not be expected to re-initiate a new propagating chain. Values of 1.67×10^{-10} L mol^{-1} s^{-1} and 1.67×10^{-8} L mol^{-1} s^{-1} were used for k_{r11} and k_{r12}, respectively, according to a previous study [10].

3.4. Termination

The termination reaction occurs by both combination and disproportionation of polymer radicals (see also Scheme 2):

$$R_i(s)^\bullet + R_j(r)^\bullet \xrightarrow{k_{tcij}} P(s+r) \tag{12}$$

$$R_i(s)^\bullet + R_j(r)^\bullet \xrightarrow{k_{tdij}} P(s) + P(r) \tag{13}$$

The overall termination rate constant of BA, $k_{t22} = k_{tc22} + k_{td22}$, was fitted to an Arrhenius expression as [17,24]:

$$k_{t22}\ (\mathrm{L\ mol^{-1}s^{-1}}) = 1.34 \times 10^9 \exp(-674/T) \quad (14)$$

The termination rate constants of Lim-related species, *i.e.*, k_{tc11}, k_{td11}, k_{tcaa}, k_{tc1a}, and k_{tc2a}, and cross-termination, *i.e.*, k_{tc12} and k_{td12}, were set to the same level as for BA radicals. Due to the lack of any known values for these parameters in the literature and because BA feed concentrations were at 50% or higher, this was considered a best option for an initial guess. The ratio of termination by combination to overall termination rate ($\frac{k_{tc}}{k_t}$), is taken as 0.9 for both the BA and Lim radicals as recommend by Peck and Hutchinson for the termination for secondary-secondary radicals [14].

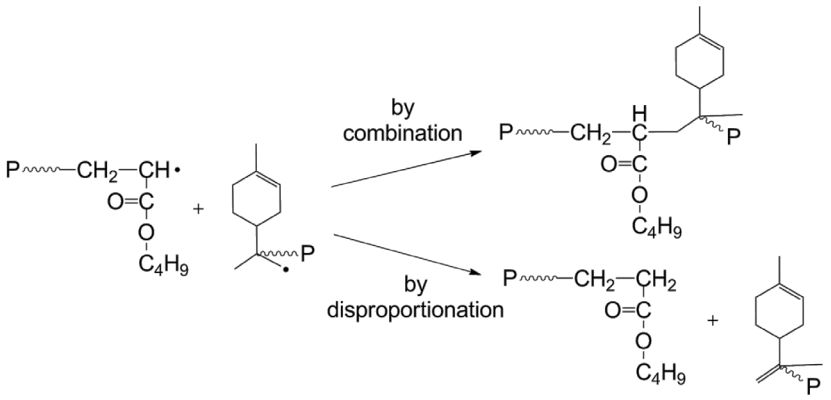

Scheme 2. Ideal reaction schematic of termination reaction of BA/Lim copolymerization.

3.5. Backbiting of BA

There is significant evidence that intramolecular chain transfer to polymer is significant during the chain propagation reaction of BA [14,25,26]. The mid-chain tertiary radicals resulting from a backbiting mechanism are quite stable and present slower propagation rates compared to the secondary radicals resulting from regular chain-end propagation. The propagation of tertiary radicals creates short-chain branches in the polymer. The backbiting and short-chain branching mechanisms were included in this model:

$$\mathrm{R_2\ (s)^\bullet} \xrightarrow{k_{bb}} \mathrm{Q_2\ (s)^\bullet} \quad (15)$$

$$\mathrm{Q_2\ (s)^\bullet} + M_i \xrightarrow{k_{p2i}{}^{tert}} \mathrm{R_i\ (s+1)^\bullet} \quad (16)$$

The symbol $\mathrm{Q^\bullet}$ represents the mid-chain tertiary radical. The rate constants for backbiting (k_{bb}) and short branching propagation ($k_{p2i}{}^{tert}$) were fitted using [16,21]:

$$k_{bb}\ (\mathrm{L\ mol^{-1}s^{-1}}) = 3.87 \times 10^6 \exp(-2299/T) \quad (17)$$

$$k_{p22}{}^{tert}\ (\mathrm{L\ mol^{-1}s^{-1}}) = 59.9 \exp(-64.2/T) \quad (18)$$

$$k_{p21}{}^{tert} = \frac{k_{p22}{}^{tert}}{r_2} \quad (19)$$

The mid-chain tertiary radical can terminate with either a tertiary radical or a chain-end secondary radical:

$$\begin{aligned} \mathrm{Q_2\ (s)^\bullet + Q_2\ (r)^\bullet} &\xrightarrow{k_{tc}{}^{tert-tert}} \mathrm{P(s+r)} \\ \mathrm{Q_2\ (s)^\bullet + Q_2\ (r)^\bullet} &\xrightarrow{k_{td}{}^{tert-tert}} \mathrm{P\ (s) + P(r)} \end{aligned} \quad (20)$$

$$\begin{aligned} Q_2\,(s)^{\bullet} + R_i\,(r)^{\bullet} &\xrightarrow{k_{tc}^{tert-sec}} P(s+r) \\ Q_2\,(s)^{\bullet} + R_i\,(r)^{\bullet} &\xrightarrow{k_{td}^{tert-sec}} P(s) + P(r) \end{aligned} \quad (21)$$

By assuming the termination rate constant for BA is independent of radical type, the overall termination rate constant of tertiary radicals is taken to be the same as k_{t22} [14,17]. Unlike secondary radicals, termination by disproportionation is favored by tertiary radicals. The ratio of termination by combination to overall termination rate was taken as 0.1 for tertiary-tertiary radicals, 0.3 for tertiary-secondary radicals [14,21], and 0.5 for tertiary-allylic radicals.

All the rate constants were assumed as chain-length independent for the purposes of model simplification. Note that diffusion-control effects were not considered in the BA/Lim kinetic model, since the polymerization temperature is much higher than the glass transition temperature of the mixture, so that the molecules are in a rubbery (mobile) state. In the BA/Lim data used in this study, conversion was kept relatively low (due to the degradative chain transfer presented by Lim) and the reaction medium was not viscous enough to induce diffusion-controlled behavior.

4. Results And Discussion

4.1. Backbiting of BA

Figure 2 shows conversion *vs.* time data and Figure 3 shows molecular weight *vs.* time data along with model predictions at f_{BA} = 0.9 with and without considering the backbiting mechanism using the initial rate constants. As the data illustrate, modeling without considering backbiting led to an overestimation of conversion results, while modeling with backbiting showed a considerable underestimation of the results. This reflects the fact that the backbiting mechanism yields tertiary radicals which exhibit a much lower reactivity, and the overall reaction rate is therefore reduced. In Figure 3, the model with backbiting provides a more reasonable prediction of the average molecular weights, whereas the model without backbiting yielded a much higher prediction. Each backbiting event results in the creation of a short branch on the main polymer chain, and the molecular weight is decreased accordingly. In order to balance the conversion and molecular weight simulation results, the rate constants of propagation for both species (BA and Lim) were adjusted to new values to present better predictions (see values in Table 2). It is important to point out that k_p for BA was estimated using the experimental data at high BA content (f_{BA} = 0.9), whereas k_p for Lim was estimated using the experimental data at low BA content (f_{BA} = 0.5).

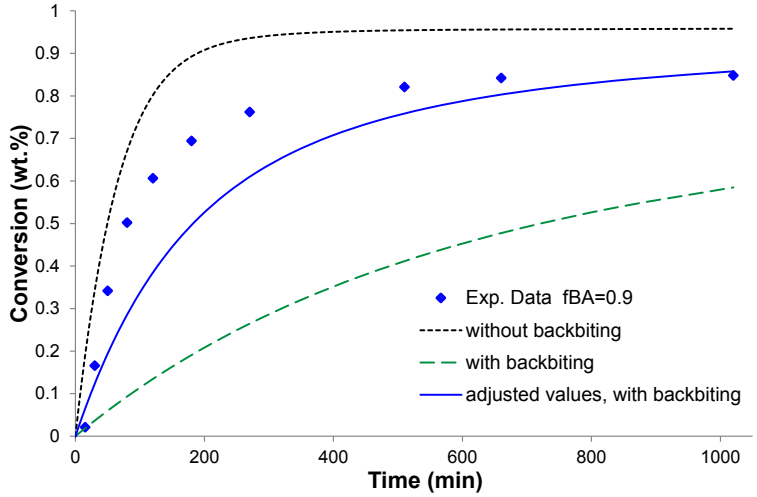

Figure 2. Conversion *vs.* time simulation with and without backbiting, BA/Lim copolymerization at feed composition f_{BA} = 0.9, at 80 °C in bulk using BPO (1 wt.%).

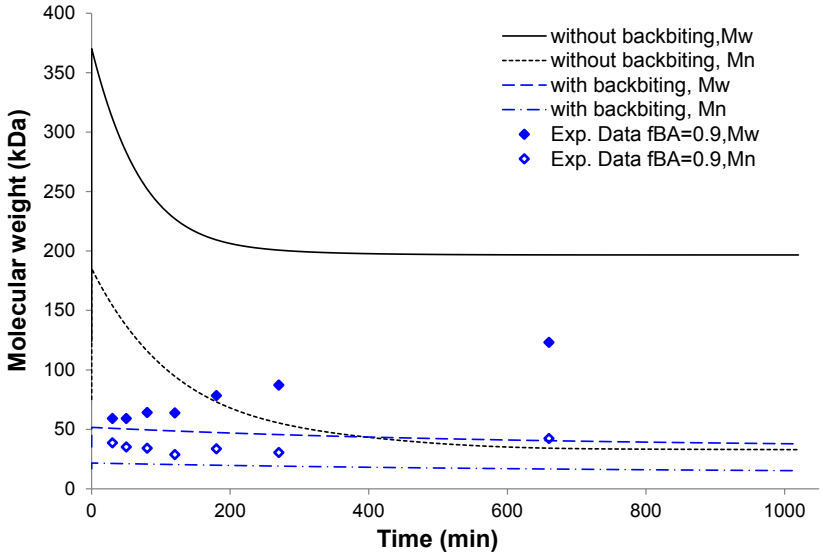

Figure 3. Molecular weight *vs.* time simulation with and without backbiting, BA/Lim copolymerization at feed composition f_{BA} = 0.9, at 80 °C in bulk using BPO (1 wt.%).

4.2. Conversion vs. Time Results

The conversion *vs.* time model predictions at five different initial feed compositions (f_{BA} = 0.5 to 0.9) along with the experimental data are shown in Figure 4. The agreement between the model and the experimental data is reasonably good. The model prediction trends in the data are well-predicted by the model; increases in BA feed content resulted in higher reaction rates. However, predictions at higher BA feed fractions were less impressive. One possible explanation could be that the degradative chain transfer reaction of Lim competes with the backbiting mechanism, as the BA chain-end radicals possibly abstracted the hydrogen from the Lim molecule rather than from an acrylate unit on its own chain. In other words, backbiting, which is the main cause for a decrease in the polymerization rate, is less dominant in the presence of Lim.

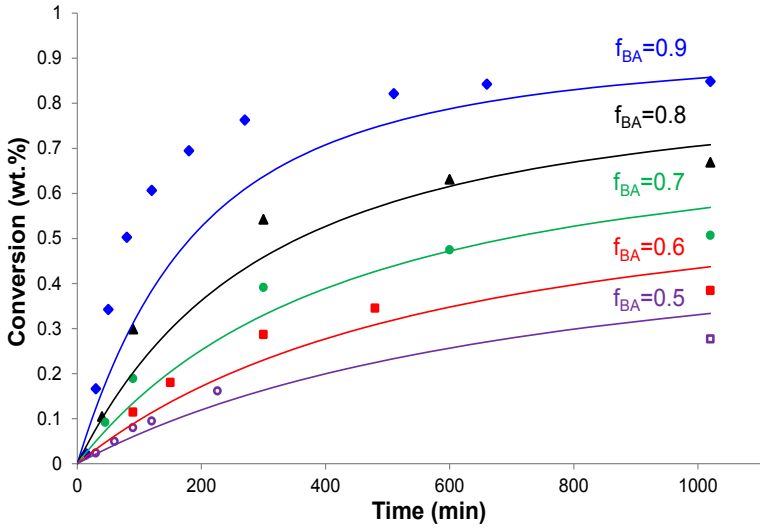

Figure 4. Conversion *vs.* time profiles for BA/Lim bulk copolymerizations at various feed compositions. Solid lines are model predictions.

4.3. Copolymer Composition vs. Conversion

Composition *vs.* conversion profiles for different feed compositions are shown in Figure 5. As mentioned earlier, the propagation rate constants were calculated using the reactivity ratios previously estimated from low-conversion BA/Lim experiments [6]. The agreement between model profiles and experimental data are in general, very good. The good predictions of the composition *vs.* conversion data validates the reactivity ratio values estimated.

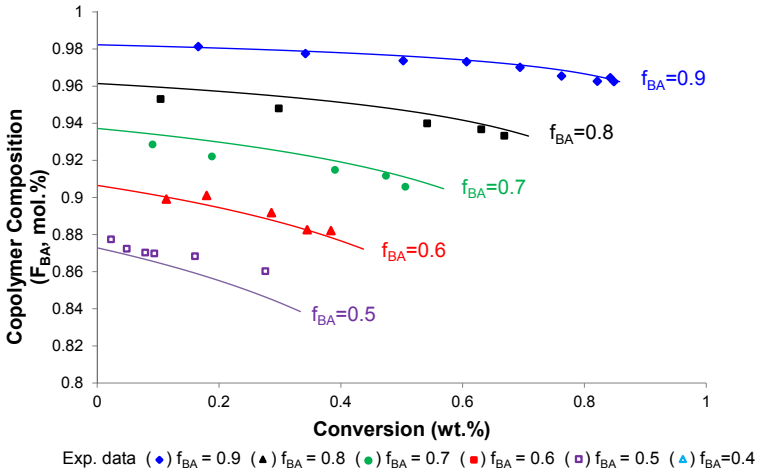

Figure 5. Composition *vs.* conversion profiles for BA/Lim copolymerizations at various feed compositions. Solid lines are model prediction.

4.4. Molecular Weight of Soluble Copolymer

Figure 6 shows plots of the molecular weight development *vs.* conversion at four different feed compositions. The number-average molecular weight (M_n) is relatively well predicted by the model but the weight-average molecular weight (M_w) shows some discrepancy. Nonetheless, good prediction of molecular weight data is often difficult to achieve. One can, however, make important conclusions about the reaction mechanisms despite some model mismatch. The model reveals that the average molecular weight decreases significantly with increasing Lim concentration in the feed. Given the propagation and chain transfer rate constants for Lim fitted to this model (see Table 2), it can be concluded that Lim acts more like a chain transfer agent than a co-monomer. One may also note that M_n decreases with increasing conversion, which is consistent with the fact that more short-chain polymers were produced. The production of increasing amounts of short-chain polymers likely resulted from increased degradative chain transfer due to increased Lim concentration as BA was preferentially incorporated into the copolymer during the early stages of the polymerization (see reactivity ratios described earlier, and Figure 5).

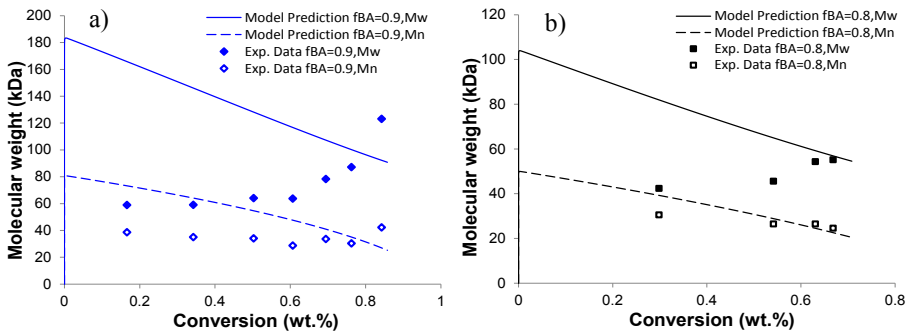

Figure 6. *Cont.*

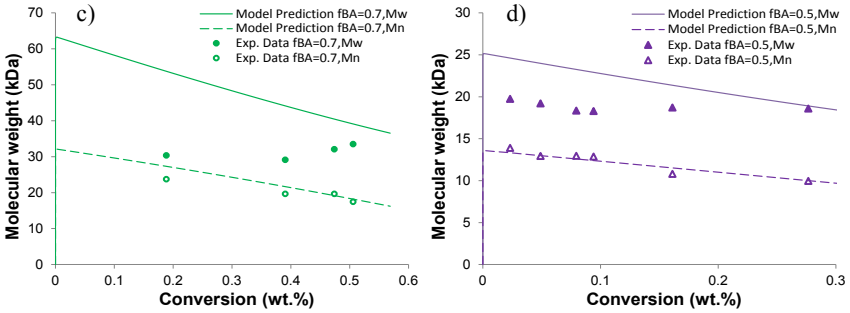

Figure 6. Molecular weight *vs.* conversion profiles for BA/Lim copolymerization at various feed compositions: (**a**) $f_{BA} = 0.9$, (**b**) $f_{BA} = 0.8$, (**c**) $f_{BA} = 0.7$, and (**d**) $f_{BA} = 0.5$.

One possible explanation for the broadening polydispersity evident from Figure 6 could relate to long-chain branching caused by the intermolecular chain transfer of BA (a propagating radical abstracts the hydrogen from an acrylate unit in the middle of another chain) [14], which can result in a significant increase in M_w. In this case, additional studies would be required to pursue these ideas further.

5. Conclusions

A kinetic model of the bulk polymerization of BA/Lim has been developed with the addition of important mechanisms for degradative chain transfer to Lim and backbiting for BA. Rate constants related to BA and Lim species were calculated based on literature values, reactivity ratios and degradative chain transfer constants estimated from previous experimental results. Fitting of the propagation rate constants resulted in moderately good conversion and molecular weight predictions and very good predictions of copolymer composition. The model supports the presence of a significant degradative chain transfer to Lim reaction as well as a backbiting mechanism for BA. Future work including a long-chain branching mechanism may shed further light on this copolymer system. In any event, this work provides greater insight into the use of an important bio-based, renewable monomer.

Acknowledgments: The authors acknowledge the support of the China Scholarship Commission for the support of Ms. Shanshan Ren. Furthermore, financial support for this project by Intellectual Ventures and the Natural Sciences and Engineering Research Council (NSERC) of Canada is greatly appreciated. E. Vivaldo-Lima acknowledges support from DGAPA-UNAM (PASPA Program) and the University of Ottawa Distinguished Visiting Researcher Program.

Author Contributions: Marc A. Dubé and Shanshan Ren conceived the experimental research. Shanshan Ren conducted all experiments and characterization. Eduardo Vivaldo-Lima performed all simulations with feedback from Shanshan Ren. Marc A. Dubé and Eduardo Vivaldo-Lima provided technical direction to the project. Shanshan Ren wrote the paper while Marc A. Dubé and Eduardo Vivaldo-Lima revised the final document.

Conflicts of Interest: The authors declare no conflict of interest.

References

1. Belgacem, M.N.; Alessandro, G. *Monomers, Polymers and Composites from Renewable Resources*; Elsevier: Amsterdam, The Netherlands, 2008; p. 543.
2. Ahmed, J.; Tiwari, B.K.; Imam, S.H.; Rao, M.A. *Starch-based Polymeric Materials and Nanocomposites: Chemistry, Processing, and Applications*; CRC Press: Boca Raton, FL, USA, 2012.
3. Kim, Y.W.; Kim, M.J.; Chung, B.Y.; Bang, D.Y.; Lim, S.K.; Choi, S.M.; Lim, D.S.; Cho, M.C.; Yoon, K.; Kim, H.S.; *et al*. Safety evaluation and risk assessment of D-limonene. *J. Toxicol. Environ. Health Pt B* **2013**, *16*, 17–38. [CrossRef] [PubMed]
4. Ciriminna, R.; Lomeli-Rodriguez, M.; Demma Cara, P.; Lopez-Sanchez, J.; Pagliaro, M. Limonene: A versatile chemical of the bioeconomy. *Chem. Commun.* **2014**, *50*, 15288–15296. [CrossRef] [PubMed]

5. Wilbon, P.A.; Chu, F.; Tang, C. Progress in renewable polymers from natural terpenes, terpenoids, and rosin. *Macromol. Rapid Commun.* **2013**, *34*, 8–37. [CrossRef] [PubMed]
6. Ren, S.; Trevino, E.; Dubé, M.A. Copolymerization of limonene with *n*-butyl acrylate. *Macromol. React. Eng.* **2015**, *9*, 339–349. [CrossRef]
7. Zhang, Y.; Dubé, M.A. Copolymerization of *n*-butyl methacrylate and D-limonene. *Macromol. React. Eng.* **2014**, *8*, 805–812. [CrossRef]
8. Zhang, Y.; Dubé, M.A. Copolymerization of 2-Ethylhexyl acrylate and D-limonene. *Polym. Plast Technol. Eng* **2015**, *54*, 499–505. [CrossRef]
9. Ren, S.; Zhang, L.; Dubé, M.A. Free-radical terpolymerization of *n*-butyl acrylate/butyl methacrylate/D-limonene. *J. Appl. Polym. Sci.* **2015**, *132*, 42821–42829. [CrossRef]
10. Zhang, Y.; Dubé, M.A.; Vivaldo-Lima, E. Modeling degradative chain transfer in D-Limonene/*n*-butyl methacrylate free-radical copolymerization. *J. Renew. Mat.* **2015**, *3*, 318–326. [CrossRef]
11. Li, D.; Grady, M.C.; Hutchinson, R.A. High-temperature semibatch free radical copolymerization of butyl methacrylate and butyl acrylate. *Ind. Eng. Chem. Res.* **2005**, *44*, 2506–2517. [CrossRef]
12. Beuermann, S.; Paquet, D.A.; McMinn, J.H.; Hutchinson, R.A. Determination of free-radical propagation rate coefficients of butyl, 2-ethylhexyl, and dodecyl acrylates by pulsed-laser polymerization. *Macromolecules* **1996**, *29*, 4206–4215. [CrossRef]
13. Lyons, R.A.; Hutovic, J.; Piton, M.C.; Christie, D.I.; Clay, P.A.; Manders, B.G.; Kable, S.H.; Gilbert, R.G. Pulsed-laser polymerization measurements of the propagation rate coefficient for butyl acrylate. *Macromolecules* **1996**, *29*, 1918–1927. [CrossRef]
14. Peck, A.N.F.; Hutchinson, R.A. Secondary reactions in the high-temperature free radical polymerization of butyl acrylate. *Macromolecules* **2004**, *37*, 5944–5951. [CrossRef]
15. Nikitin, A.N.; Hutchinson, R.A. Effect of intramolecular transfer to polymer on stationary free radical polymerization of alkyl acrylates, 2. *Macromol. Theory Simul.* **2006**, *15*, 128–136. [CrossRef]
16. Rantow, F.S.; Soroush, M.; Grady, M.C.; Kalfas, G.A. Spontaneous polymerization and chain microstructure evolution in high-temperature solution polymerization of *n*-butyl acrylate. *Polymer* **2006**, *47*, 1423–1435. [CrossRef]
17. Nikitin, A.N.; Hutchinson, R.A.; Buback, M.; Hesse, P. Determination of intramolecular chain transfer and midchain radical propagation rate coefficients for butyl acrylate by pulsed laser polymerization. *Macromolecules* **2007**, *40*, 8631–8641. [CrossRef]
18. Gao, J.; Penlidis, A. A Comprehensive simulator/database package for reviewing free-radical homopolymerizations. *J. Macromol. Sci. Part C* **1996**, *36*, 199–404. [CrossRef]
19. Gao, J.; Penlidis, A. A Comprehensive simulator/database package for reviewing free-radical copolymerizations. *J. Macromol. Sci. Part C* **1998**, *38*, 651–780. [CrossRef]
20. Gao, J.; Penlidis, A. A Comprehensive simulator/database package for bulk/solution free-radical terpolymerizations. *Macromol. Chem. Phys.* **2000**, *201*, 1176–1184. [CrossRef]
21. Dorschner, D. Multicomponent Free Radical Polymerization Model Refinements and Extensions with Depropagations. Master's Thesis, University of Waterloo, Department of Chemical Engineering, Waterloo, ON, Canada, 2010.
22. Asua, J.M.; Beuermann, S.; Buback, M.; Castignolles, P.; Charleux, B.; Gilbert, R.G.; Hutchinson, R.A.; Leiza, J.R.; Nikitin, A.N.; Vairon, J.; *et al*. Critically evaluated rate coefficients for free-radical polymerization, 5. *Macromol. Chem. Phys.* **2004**, *205*, 2151–2160. [CrossRef]
23. Jun, W. Mathematical Modeling of Free-Radical Six Component Bulk and Solution Polymerization. Master's Thesis, University of Waterloo, Department of Chemical Engineering, Waterloo, ON, Canada, 2008.
24. Beuermann, S.; Buback, M. Rate coefficients of free-radical polymerization deduced from pulsed laser experiments. *Prog. Polym. Sci.* **2002**, *27*, 191–254. [CrossRef]
25. Plessis, C.; Arzamendi, G.; Leiza, J.R.; Schoonbrood, H.A.S.; Charmot, D.; Asua, J.M. modeling of seeded semibatch emulsion polymerization of *n*-BA. *Ind. Eng. Chem. Res.* **2001**, *40*, 3883–3894. [CrossRef]
26. Ahmad, N.M.; Heatley, F.; Lovell, P.A. Chain transfer to polymer in free-radical solution polymerization of *n*-butyl acrylate studied by NMR spectroscopy. *Macromolecules* **1998**, *31*, 2822–2827. [CrossRef]